View metadata, citation and similar papers at core.ac.uk

brought to you by CORE

provided by Elsevier - Publisher Connector

Alexandria Engineering Journal (2015) 54, 405–413

HOSTED BY

ELSEVIER

Alexandria University

Alexandria Engineering Journal

www.elsevier.com/locate/aej
www.sciencedirect.com

ORIGINAL ARTICLE

Combustion characteristics of lemongrass (*Cymbopogon flexuosus*) oil in a partial premixed charge compression ignition engine

Avinash Alagumalai *

Internal Combustion Engineering, Department of Mechanical Engineering, Sri Venkateswara College of Engineering, Sriperumbudur 602117, India

Received 17 December 2014; revised 23 March 2015; accepted 31 March 2015
Available online 5 June 2015

KEYWORDS

Lemongrass oil;
Cylinder pressure analysis;
Heat-release analysis

Abstract Indeed, the development of alternate fuels for use in internal combustion engines has traditionally been an evolutionary process in which fuel-related problems are met and critical fuel properties are identified and their specific limits defined to resolve the problem. In this regard, this research outlines a vision of lemongrass oil combustion characteristics. In a nut-shell, the combustion phenomena of lemongrass oil were investigated at engine speed of 1500 rpm and compression ratio of 17.5 in a 4-stroke cycle compression ignition engine. Furthermore, the engine tests were conducted with partial premixed charge compression ignition-direct injection (PCCI-DI) dual fuel system to profoundly address the combustion phenomena. Analysis of cylinder pressure data and heat-release analysis of neat and premixed lemongrass oil were demonstrated in-detail and compared with conventional diesel. The experimental outcomes disclosed that successful ignition and energy release trends can be obtained from a compression ignition engine fueled with lemongrass oil.

© 2015 Faculty of Engineering, Alexandria University. Production and hosting by Elsevier B.V. This is an open access article under the CC BY-NC-ND license (http://creativecommons.org/licenses/by-nc-nd/4.0/).

1. Introduction

Energy utilization is unavoidable in every human life. There are several reasons for choosing alternative fuels instead of fossil fuels. In fact, the energy demand occurs due to two major disputes, one is the rapid increase in global population and the second is increasing cost of fossil fuels. In the last few years, a major attention has been given to use biodiesel as an alternative fuel for transportation system in order to address the challenges of increasing diesel prices and fast depletion of easily accessible fossil fuel reserves [1–5].

In recent days, developed countries such as the United States, France, Germany and England, and also developing countries such as Argentina, Brazil, Malaysia, Indonesia and India have shown their interest for expanding and producing renewable energy fuels with some government financial aids. This interest can be attributed to the commonly seen advantages of biofuels, particularly a substantial decrease in vehicle emissions. Canada and European Union (EU) have already started

* Address: Internal Combustion Engineering, Department of Mechanical Engineering, Sri Venkateswara College of Engineering, Sriperumbudur 602117, Tamil Nadu, India. Mobile: +91 8012645399.
E-mail address: avinashandromeda@gmail.com

Peer review under responsibility of Faculty of Engineering, Alexandria University.

http://dx.doi.org/10.1016/j.aej.2015.03.021
1110-0168 © 2015 Faculty of Engineering, Alexandria University. Production and hosting by Elsevier B.V.
This is an open access article under the CC BY-NC-ND license (http://creativecommons.org/licenses/by-nc-nd/4.0/).

this replacement at a certain percent for decreasing green house emissions. By 2020 the European parliament would increase the biofuel market share of about 10%. Also, the Canadian government has announced the use of 5% heated biodiesel in the place of diesel in transportation sector by 2015 [6].

As Reported by Alenezi et al. [7] biodiesel is one of the significant biofuels in the EU, which comprises 80% of the total biofuel production. In EU around 4 million hectares of arable land is used for producing biodiesel. Also, across the EU approximately 40 biodiesel production plants are located and their production capacities are growing rapidly. To proceed further, the United States is presently setting a new target to cut greenhouse gas emissions to about 26–28% below 2005 levels by 2025. And, the current target of the country is to reach a level of 17% below 2005 emissions by 2020. Also, China, which is the world's largest greenhouse-gas emitter agreed to increase its share on non-fossil fuels of energy production to about 20% by 2030 [8].

In actual fact, a number of vegetable oils have been tested all over the world to assess their performance in diesel engines. Even though straight vegetable oil can be used as a sole fuel, it is a bitter truth that esterified oil shows better fuel properties [9,10]. This is due to the fact that vegetable oils exhibit high viscosity than diesel. Also, a limitation on the use of biodiesel is its cost. Besides, in the present market the price of biodiesel is higher than that of diesel. In this regard, an in-edible vegetable oil with comparable fuel properties to diesel would stimulate a curiosity to do research. By the way, lemongrass oil (LGO) is one among those vegetable oils which exhibits fairly closer properties to conventional diesel.

In this work, plant species lemongrass (*Cymbopogon flexuosus*) is discussed as a newer source of fuel for diesel engine. Lemongrass is one of the essential oil plants widely grown in the tropics and subtropics of Africa, Indonesia, India, Madagascar, and South America. In India, it is cultivated along Western Ghats (Maharashtra and Kerala), Tamil Nadu and Karnataka, and also foot-hills of Arunachal Pradesh and Sikkim; i.e., it can be cultivated on widespread range throughout India and may favor easy availability [11]. Furthermore, lemongrass is a high-biomass crop that may have applications for biofuel production. Owing to the content of its high-value essential oil, the cost for production of biofuel may be low, since the biomass would be a by-product of essential oil production. Lemongrass may demonstrate to be a new high-value specialty crop and a worthy source for biofuel in the southeastern United States (a region known for its hot and humid climate) [12].

Over the last decade, automotive engineers have been struggling to substantially reduce the engine out exhaust emissions in order to meet the upcoming stringent exhaust regulations. In this regard, an alternative engine technology, most commonly known as homogenous charge compression ignition (HCCI) has emerged that has a potential to accomplish lower magnitude of NO_x and virtually no smoke emissions [13]. Besides, in this new combustion process, premixed fuel–air mixture and auto-ignited combustion are the two fundamental characteristics. Although potential benefits are noted with this new combustion process, challenges such as combustion phasing control, extension of operation, cold start problem, high combustion noise, and high HC and CO emissions disclose that further experimental exploration is essentially needed in this area.

After a critical review of literature, an endeavor has been made here to study in detail the combustion characteristics of neat and premixed LGO in a single-cylinder air-cooled compression ignition (CI) engine operated at a maximum load of 3.3 kW and standard injection timing of 23° BTDC.

2. Materials and methods

In this study, in order to understand the effects of LGO usage in CI engine, in-cylinder gas pressure traces were examined. Although an in-depth explanation of the combustion process in diesel engine is extremely difficult due to unsteady liquid jet phenomena and mixture of non-uniformity, some useful data to highlight and explain the combustion characteristics of LGO are presented in this work. This was done with an aid of high-resolution data acquisition system.

For the present work, an AVL combustion analyzer attached with AVL INDIMICRA 602-T10602A was used for combustion diagnosis. The signals from AVL/GH 14D/AH01 pressure transducer were converted into voltage signals with a help of a charge amplifier. The specifications of the AVL pressure transducer are given in Table 1. In the present case, an endeavor has been made to investigate PCCI-DI dual fuel concept. In PCCI-DI mode, well atomized LGO was injected very close to the intake port using an auxiliary injector and direct injection of diesel by main injector as usual. And, in PCCI-DI mode, the intake air temperature was maintained at 40 °C by an electric heater to enhance the fuel atomization rate. Also, the premixed fuel injected was precisely timed just after the intake valve opening in order to reduce the wall wetting issues. The quantity of premixed fuel to be injected for different premixed ratios (5% and 10%) was calculated based on energy basis using the following expression (1):

$$r_p = \frac{m_p h_p}{m_p h_p + m_d h_d} \tag{1}$$

where r_p is the premixed ratio, m_p the mass of premixed fuel, m_d the mass of direct injected fuel, h_p the lower heating value of premixed fuel, and h_d is the lower heating value of direct injected fuel.

To proceed further, in the present case, 10% premixed ratio has been used as the maximum premix fraction for LGO. This is because the heating value of premixed fuel (LGO) used is less when compared to diesel. Therefore, on energy basis the quantity of premixed fuel to be injected increases exponentially with increasing premixing ratios. Also, to limit the maximum rate of pressure rise during PCCI-DI mode, all experiments were conducted up to 3.3 kW load.

The cylinder pressure and other signals picked up by various transducers were collected by the system for 50 consecutive engine cycles. The test engine setup is shown in Fig. 1, the engine specifications are provided in Table 2, and the fuel

Table 1 Specifications of the AVL pressure transducer.

Sensitivity	=	18.99 pC/bar
Linearity	< ±	0.30%
Measuring range	=	0 to 250 bar
Operating temperature range	=	−40 to 400 °C
Natural frequency	=	115 kHz

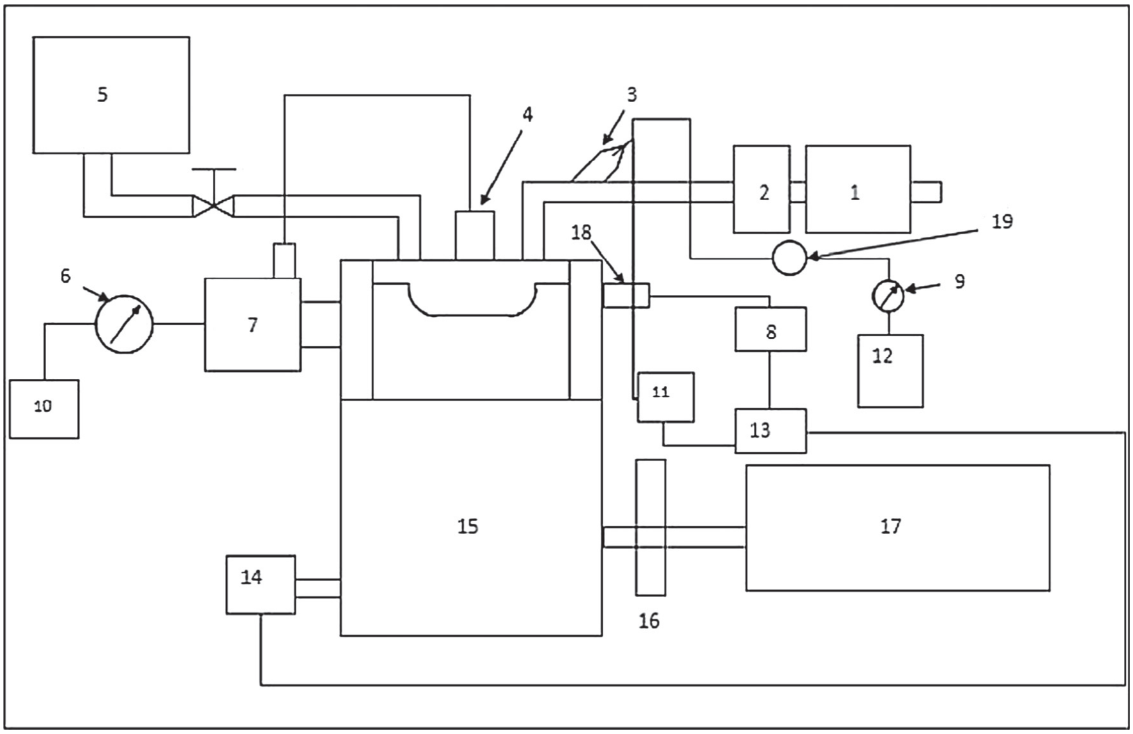

1-Air surge tank	11- Relay and temperature controller
2-Electric heater	12-Port fuel tank
3-Auxillary fuel injector	13-Data acquisition
4-Main fuel injector	14-Crank angle encoder
5-Exhaust gas analyzer	15-Engine
6-Flow meter	16-Flywheel
7-Fuel injector pump	17-Dynamometer
8-Charge amplifier	18-Pressure Transducer
9-Flow meter	19-Fuel control valve
10-Main fuel tank	

Figure 1 Experimental setup.

properties of LGO and neat diesel are distinguished in Table 3. The measured cylinder pressure and other operating parameters were used to calculate rate of pressure rise, heat-release rate, cumulative heat-release rate, ignition delay, combustion duration, and mass fraction burned.

3. Results and discussion

3.1. Analysis of cylinder pressure data

3.1.1. Linear p–V and log p–V

Generally, cylinder pressure changes with crank angle as a result of cylinder volume change, combustion, heat transfer to the combustion chamber walls, flow into and out of crevice regions and leakage. The first two of the above said effects are the largest. Furthermore, the effect of volume change on the pressure can readily be accounted for; thus, combustion rate information can be obtained from accurate data provided models for the remaining phenomena can be developed at an appropriate level of approximation [13,14].

Table 2 Test engine specifications.

Make	Kirloskar TAF1
Type	Four stroke, single cylinder vertical air cooled diesel engine
Rated power	4.4 kW
Rated speed	1500 rpm
Bore	87.5 mm
Stroke	110 mm
Compression ratio	17.5:1
Orifice diameter	13.6 mm
Coefficient of discharge	0.6
Port fuel injection	4.5° BTDC
Port fuel injection pressure	3.5 bar

The cylinder pressure and corresponding cylinder volume throughout the engine operating cycle can be plotted on a linear p–V and a log p–V diagram as shown in Figs. 2 and 3.

Table 3 Fuel properties.

Properties	Lemongrass oil	Diesel
Cetane number	45	50–55
Heating value (kJ/kg)	36,000	42,500
Density (kg/m^3)	910	860
Flash point (°C)	50	55
Kinematic viscosity @ 40 °C (Cst)	4.1	3.2

Fig. 2 shows the sequence of processes which make up a typical CI engine operating cycle fueled with diesel, neat and premixed LGO. The cycle can be divided into suction, compression, combustion, expansion, and exhaust processes. On the *p–V* diagram, one can see that the enclosed area of diesel is more when compared to neat LGO. This trend clearly indicates that work per cycle is more for diesel fuel operation than neat LGO. The primary reason for this trend is low heating value and slightly high viscosity of neat LGO when compared to diesel. Therefore, a large amount of energy might have released during the combustion of diesel than neat LGO. And, in case of PCCI-DI mode, the work per cycle increased for premixed LGO when compared to neat LGO. However, the maximum work per cycle decreased with increasing premixed fraction. This is due to the fact that some of the air is replaced by the fuel addition during the induction stroke in case of higher premixed ratio.

Furthermore, log *p–V* plot can be used to check the quality of cylinder pressure data. On the log *p*–log *V* diagram (see Fig. 3) the compression process is a cured line. Also, on the plot the start of combustion can be identified by the departure of the curve from the compression curve. In similar fashion,

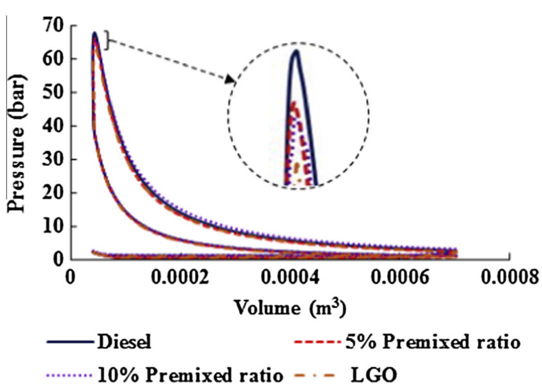

Figure 2 Linear *p–V* diagram.

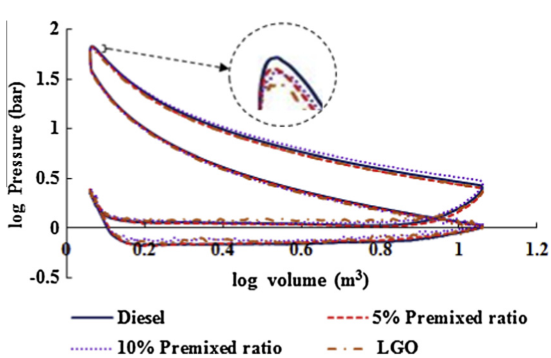

Figure 3 Log *p–V* diagram.

the end of combustion can be located approximately. Like compression process, the expansion process is also a curved line. The compression and expansion processes of both diesel and LGO can be fitted well by a polytropic relation (pv^n = constant). Overall, the start and end of combustion of diesel, premixed and neat LGO can be approximately defined on the log *p–V* plot.

3.1.2. Cylinder gas pressure

Cylinder pressure versus crank angle data over the compression and expansion processes of the engine operating cycle can be used to obtain quantitative information on the progress of combustion [14]. The variation of cylinder pressure versus crank angle for diesel, premixed and neat LGO at maximum load of 3.3 kW is shown in Fig. 4. In CI engine, cylinder pressure depends on the burned fuel fraction during the premixed burning phase (i.e., the initial stage of combustion). This stage of combustion depends upon the ability of the fuel to mix well with air and burn [14,15]. In this work, the peak cylinder pressure obtained is higher for diesel (67.836 bar) followed by 5% premixed LGO (66.144), 10% premixed LGO (65.626) and neat LGO (64.157 bar). The maximum cylinder pressure of neat LGO is comparatively less when compared to the maximum cylinder pressure of diesel at the same operating condition. The reason for this reduced pressure is the lower calorific value and slightly higher viscosity of neat LGO compared to diesel. The other possible reason is a significantly large amount of energy released during the combustion of diesel, while neat LGO showed a slightly slow burning rate.

In case of PCCI-DI mode, the pressure profiles of 5% and 10% premixed fractions remain more or less constant. However, for 10% premixed fraction, the peak pressure slightly reduced when compared to 5% rate. This drop in pressure is primarily due to the drop in the amount of air entering the cylinder with an increasing premixing ratio. Furthermore, from Fig. 4 the point at which the pressure curves of diesel, premixed and neat LGO separate from the motoring (non-firing) curve provides information on the start of combustion. The corresponding values of start of combustion (in crank angle degree) of diesel, 5% premix fraction, 10% premix fraction and neat LGO are −6.64, −7.42, −6.65 and −6.82, respectively.

3.1.3. Rate of pressure rise

Fig. 5 shows the rate of pressure rise characteristics of diesel, premixed and neat LGO at maximum load condition. The rate of pressure rise is often used as a measure of combustion

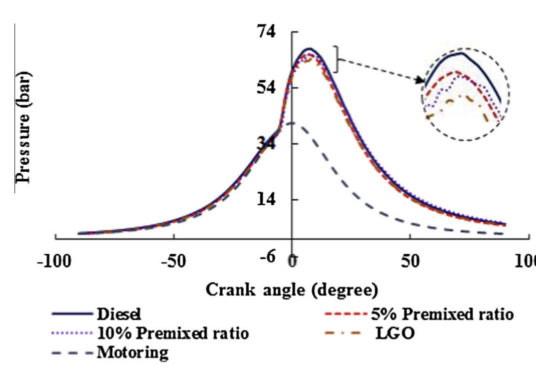

Figure 4 Pressure versus crank angle diagram.

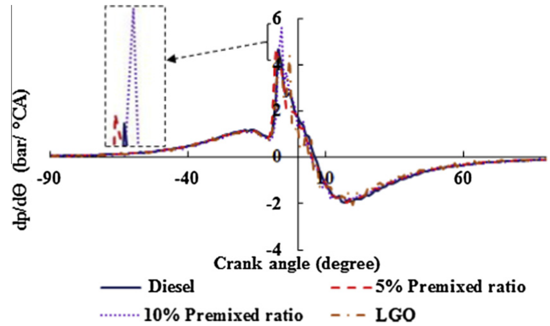

Figure 5 Rate of pressure rise.

generated noise. However, the acceptable limit for maximum rate of pressure rise is subjective [13]. It is apparent from the plot that neat LGO shows lower rate of pressure rise as compared to diesel fuel due to lower ignition delay. As a result, premixed combustible mixture would make less fuel to be burned in the premixed burning phase. The major reasons for the less premixed combustible mixture are higher viscosity and lower volatility of neat LGO as compared to that of diesel fuel [15]. Because of this, the in-cylinder gas pressure and rate of pressure rise decreased for neat LGO. Even though the combustion rate is slow for PCCI-DI combustion, the rate of pressure rise is much higher than that of diesel combustion, particularly for 10% premixed fraction. Therefore, future efforts should be undertaken to decrease the rate of pressure rise. Also, from the test, the maximum rate of pressure rise was 5.594 bar/°CA occurring at 6 °CA BTDC for 10% premixed fuel. On the other hand, the minimum rate of pressure rise was 4.388 bar/°CA occurring at 3 °CA BTDC for neat LGO.

3.1.4. Maximum pressure analysis

Fig. 6 shows the variation of maximum cylinder pressure of diesel, premixed and neat LGO for 50 consecutive engine cycles. It is apparent from the plot that the maximum cylinder pressure of diesel is higher than the maximum cylinder pressure value obtained for neat LGO. Moreover, in case of PCCI-DI mode, the maximum cylinder pressure values decreased when compared to diesel. In addition, the maximum pressure analysis of PCCI-DI concept disclosed that the fuel atomization and the level of premixing decrease with increasing premix fuel quantity. A statistical model (regression model) was developed to corroborate the above statement. The predicted peak pressure values based on the developed model are provided in Table 4. The developed model too proved that the peak pressure value decreases with increasing premix fractions.

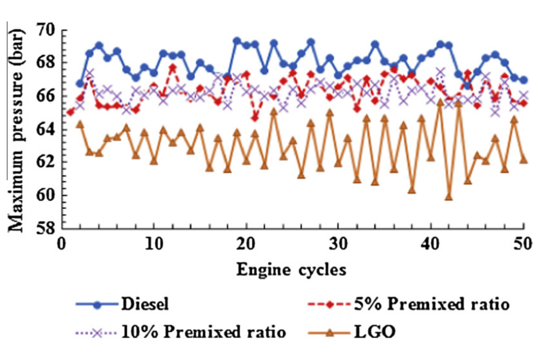

Figure 6 Maximum pressure versus engine cycles.

Furthermore, the minimum, maximum and mean values of maximum cylinder pressure of diesel, premixed and neat LGO for 50 engine cycles are listed in Table 5. Additionally, from Table 5 one can figure out the standard deviation (Std) and coefficient of variance (CoV) values of diesel, premixed and neat LGO. The standard deviation data of diesel (0.83), 5% premixed ratio (0.79) and 10% premixed ratio (0.58) project that the maximum cylinder pressure values tend to be very close to the mean, whereas for neat LGO (1.4) the standard deviation data project that the maximum cylinder pressure values are spread out over a large range of values. Likewise, the CoV (ratio of std to mean) data disclose that the CoV of neat LGO is more when compared to the other three (see Table 5).

3.2. Heat-release analysis

To investigate further the combustion phenomena of diesel, premixed and neat LGO, heat-release analysis was carried out by a simplified thermodynamic model. The heat-release diagram is a quantitative description of timely burning of fuel in an engine. It has a major effect on cycle efficiency and maximum cylinder pressure. The heat-release model used in this study is based on the first law heat-release model (see Eq. (2)). Also, in this work two polytropic coefficients have been used to develop the model. This is because the polytropic coefficient (K) depends on temperature and if the heat-release is calculated using a constant polytropic coefficient, the integral heat-release might still rise slightly even after the end of combustion has been reached. This causes inaccuracies in the calculation of mass fraction burned. Thus, a second coefficient for calculation after TDC (expansion process) has to be used. By setting the second co-efficient to a value which is

Table 4 Predicted peak pressure (bar) for new observations (confidence interval: 95).

r_p (%)	Fit	Standard error of fit
15	65.0021	0.1727
20	64.0774	0.2485
25	63.1527	0.3263
30	62.228	0.4049
35	61.3033	0.484

Regression equation: $P_{max} = 67.7763–0.184942\ r_p$.

Table 5 Maximum pressure ($P_{\max}$) analysis of diesel, premixed LGO and neat LGO.

	Diesel	5% Premixed ratio	10% Premixed ratio	LGO
Min	66.636	64.682	64.982	59.91
Mean	68.036	67.764	67.462	62.99
Max	69.34	66.346	66.189	65.63
Std	0.834	0.788	0.584	1.4
CoV	0.012	0.012	0.009	0.022

slightly smaller than the one used before TDC (compression process), one can ensure that the heat-release integral does not rise further after the end of combustion. This allows for a more accurate calculation of the end of combustion.

From the first law of thermodynamics, the apparent net heat-release rate is given by

$$\frac{dQ}{d\theta} = \frac{K}{K-1} P \frac{dV}{d\theta} + \frac{1}{K-1} V \frac{dP}{d\theta} \tag{2}$$

The piston cylinder volume or instantaneous volume of cylinder (V) can be determined as a function of crank angle from the compression ratio, bore, stroke, and connecting rod length by Slider-Crank Model. The instantaneous volume of cylinder (V) is given by equation (3) as follows:

$$V = \frac{Vd}{r-1} + \frac{Vd}{2}\left[1 + R - \cos\theta - \left(R^2 - \sin^2\theta\right)^{1/2}\right] \tag{3}$$

where V_d is the displacement volume, r the compression ratio, and R the stroke-to-bore ratio.

Furthermore, from heat-release analysis various combustion parameters such as cumulative heat-release rate, ignition delay, overall combustion duration, and mass fraction burned can be identified. Also, the start of combustion can be calculated from the heat-release curve. It can be clearly seen from the heat-release plot (see Fig. 7) that the heat-release curve dips into the negative range before its steep rise. The subsequent zero transition is taken as the start of combustion.

3.2.1. Instantaneous heat-release rate

Fig. 7 shows the variation of instantaneous heat-release rate with crank angle for diesel, premixed and neat LGO at a maximum load of 3.3 kW. The fuels experienced a rapid premixed burning followed by diffusion combustion, as it is typical for naturally aspirated engines. After the ignition delay period, the premixed fuel air mixture burned rapidly, releasing heat at a very rapid rate, after which diffusion combustion has taken place. This shows that the burning rate is controlled by the availability of combustible fuel–air mixture [16]. And, by analyzing the diagram it can be observed that the heat-release rate is higher for premixed LGO than diesel. This trend apparently reveals that the rate of pressure rise is proportional to the rate of heat release. On the other hand, neat LGO showed lower rate of heat-release. Therefore, it is obvious that use of neat LGO as sole fuel changes the combustion pattern notably (i.e., the peak of the heat-release curve of neat LGO is lower than that of diesel). This discloses that the premixed combustion region is lesser for neat LGO. Although maximum work per cycle is reduced for neat LGO, the combination of slower rate of heat-release and lower maximum rate of pressure rise might contribute to lower mechanical stress in the crank drive when compared to neat diesel operation. Therefore, low combustion noise can be achieved with neat LGO operation. These findings appeared to agree with the literature review of Agarwal [17] and Babu and Devaradjane [18].

3.2.2. Cumulative heat-release rate

Fig. 8 shows the variation of cumulative heat-release rate of diesel, premixed and neat LGO at maximum load condition. The cumulative heat-release rate is calculated by the equation (4) as follows:

$$Q_{\text{Cumulative}} = \int dQ = \int P\frac{K}{K-1}dV + V\frac{1}{K-1}dP \tag{4}$$

Initially, a negative cumulative heat-release curve is seen due to ignition delay and the curve becomes positive once the combustion is initiated. Also, from Fig. 8 the combustion timing information can be extracted by calculating 50% accumulated heat release (CA 50) where half the combustion has taken place. In general, CA 50 is normally used as a very consistent measure of combustion phasing. This is because the cumulative heat-release reaches its maximum value at or near 50% mass fraction burned, whereas the heat release values are much lower and potential crank angle error is much higher for lower burning rates [13]. In PCCI-DI mode, the CA 50 advances with increasing premix fraction. This trend reveals that the space restriction encountered in the intake manifold confines the space available for the fuel jet to travel, at higher fuel content, before it is entrapped by the air. As a result, with increasing fuel quantity being injected into the intake manifold, issues such as wall impingement come into picture and this has a pronounced impact on engine combustion.

3.2.3. Ignition delay

Ignition delay is an important parameter in combustion phenomenon. Table 6 shows the variation of ignition delay (both in angle and time) for diesel, premixed and neat LGO at different loads. In general, the angle (degree) can be converted to time (ms) by the following expression:

$$t\ (\text{ms}) = \frac{{}^{\circ}\text{CA}}{N \cdot \left(\frac{\text{min}}{60\ \text{s}}\right) \cdot \left(\frac{360^{\circ}}{\text{rev}}\right)} \cdot 1000$$

The delay period or ignition delay mentioned here refers to the time difference between the start of injection and start of combustion, that is, time interval during which each fuel

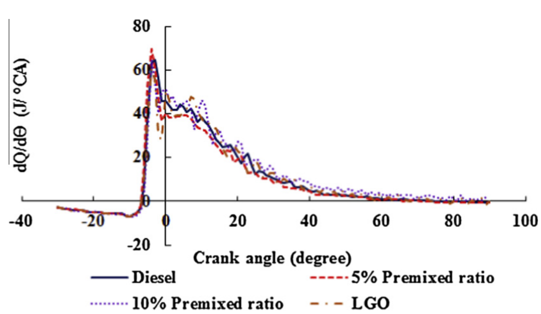

Figure 7 Heat release rate.

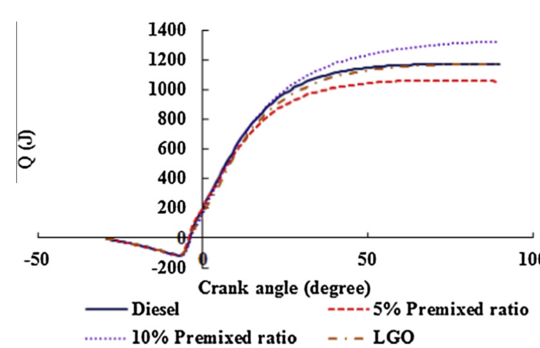

Figure 8 Cumulative heat release rate.

Table 6 Ignition delay characteristics of diesel, premixed LGO and neat LGO.

Load (%)	Ignition delay (°CA)	Ignition delay (ms)
Diesel		
0	18.14	2.015555556
25	17.2	1.911111111
50	16.88	1.875555556
75	16.36	1.817777778
5% premixed ratio		
0	17.83	1.981111111
25	17.1	1.9
50	16.43	1.825555556
75	16.15	1.794444444
10% premixed ratio		
0	18.1	2.011111111
25	18.1	2.011111111
50	17.45	1.938888889
75	16.49	1.832222222
LGO		
0	19.55	2.172222222
25	17.15	1.905555556
50	16.43	1.825555556
75	16.18	1.797777778

Table 7 Overall burn duration of diesel, premixed LGO and neat LGO.

Load (%)	Combustion duration (°CA)	Combustion duration (ms)
Diesel		
0	28.98	3.22
25	32.11	3.567777778
50	34.7	3.855555556
75	38.92	4.324444444
5% premixed ratio		
0	28.29	3.143333333
25	32	3.555555556
50	35.16	3.906666667
75	38.78	4.308888889
10% premixed ratio		
0	32.9	3.655555556
25	33.47	3.718888889
50	36.32	4.035555556
75	46.97	5.218888889
LGO		
0	30.09	3.343333333
25	33.35	3.705555556
50	37.11	4.123333333
75	42.13	4.681111111

droplet gets ready for combustion. This period is generally determined from the change in slope of the pressure versus crank angle diagram or from the heat-release analysis. The time delay decides the quantity of premixed flame. The rate of pressure rise, peak pressure, engine noise, vibrations and mechanical stress also depend on the ignition delay [19]. In general, a lot of parameters such as fuel type and quality, air–fuel ratio, engine speed, fuel atomization, intake air pressure and temperature influence the ignition delay. Among these, the fuel type is an important parameter affecting the delay period [20]. It can be observed from the table (see Table 6) that the ignition delay decreases with increase in the engine load as a result of increased cylinder gas temperature [21]. It is also apparent from the table that the ignition delay of diesel is longer than that of premixed LGO (particularly 5%) and neat LGO in the entire engine operation. In spite of the slightly higher viscosity of LGO, the ignition delay appears to be lower for premixed and neat LGO than for diesel. The primary reason may be the complex and rapid preflame chemical reaction that takes place at high temperatures. As a result of the high cylinder gas temperature, LGO has undergone thermal cracking and lighter compounds might have been produced, which might have ignited earlier to result in a shorter delay period. Generally, the increase in fuel viscosity, principally for petroleum derived fuels, results in poor atomization and mixing, increased penetration and reduced flame cone angle [22]. These factors primarily result in longer ignition delay. But, LGO is not derived from crude petroleum, and a reverse trend is seen in the case of premixed LGO and neat LGO.

3.2.4. Combustion duration

The variation of combustion duration of diesel, premixed and neat LGO at a maximum load of 3.3 kW is given in Table 7. The combustion duration was calculated based on the duration between the start of combustion and 90% cumulative heat release. The combustion duration increases with increase in load. It is clearly seen from the table that the combustion duration is more for premixed LGO (particularly 10%) and neat LGO. In case of neat LGO, the combustion duration is longer than diesel due to increase in quantity of LGO injected at maximum load when compared to diesel. The other possible reason is lower calorific value and slightly higher viscosity of LGO; it might have led to poor mixture formation compared to diesel. The results agreed with the findings of Senthil kumar et al. [23], Nazar et al. [24], and Banapurmath et al. [25]. On the other hand, the combustion duration of 10% premixed LGO is longer than neat diesel and 5% premixed LGO. This might be due to the loss of volumetric efficiency with increase in premixed fraction.

3.2.5. Mass fraction burned

The information of crank position with respect to the start and end of combustion processes can be gained by mass fraction burned analysis. The angular position of the maximum of the differential heat-release curve (i.e., mass fraction burned per °CA) as well as four mass fraction burned levels (5%, 10%, 50% and 90%) are determined and given in Table 8. The mass fraction burned thresholds are presented in %. The 90% of mass fraction burned is taken to be the end of combustion. From Table 8 it is clear that the combustion of premixed LGO and neat LGO starts earlier and the overall burn duration was more when compared to diesel. This trend proves convenient to use these mass fraction burned profiles to characterize different stages of CI engine combustion process by their duration in crank angles, thereby defining the fraction of engine cycle that they occupy.

Furthermore, the experimental mass fraction burned profiles were fitted with the Wiebe function (see Eq. (5)) by

Table 8 Mass fraction burned analysis of diesel, premixed LGO and neat LGO.

	CA0	CA5	CA10	CA50	CA90
Diesel					
Min	−6.8	−2.85	−1.9	8.75	28.25
Mean	−6.64	−2.38	−1.3	9.74	32.28
Max	−6.25	−1.65	−0.5	10.6	35.65
Std	0.127	0.208	0.317	0.432	1.22
CoV (%)	−1.91	−8.73	−24.5	4.44	3.79
5% Premixed ratio					
Min	−7	−3.3	−2.65	7.8	28.2
Mean	−6.85	−2.93	−1.89	9.14	31.93
Max	−6.6	−2.3	−0.95	10.1	36.6
Std	−0.085	0.257	0.39	0.575	2.29
CoV (%)	−1.24	−8.79	−20.66	6.29	7.16
10% Premixed ratio					
Min	−6.8	−2.65	−1.6	10.85	38.05
Mean	−6.51	−2.03	−0.688	12.14	40.43
Max	−5.95	−1.45	0.05	13.15	43
Std	0.187	0.273	0.358	0.377	1.37
CoV (%)	−2.87	−13.48	−52.03	3.11	3.4
LGO					
Min	−7.25	−2.95	−1.8	9.75	32.1
Mean	−6.82	−2.2	−0.938	10.77	35.31
Max	−6.55	−1.55	−0.25	12.1	39.75
Std	0.164	0.275	0.392	0.62	2.24
CoV (%)	−2.41	−12.51	−41.76	5.76	6.34

CA – Crank angle; 0, 5, 10, 50 and 90 are mass fractions burned (in %).

defining form factor as function of CA 10 and CA 90 (see Eq. (6)). Fig. 9(a and b) shows the plots of mass fraction burned (MFB) and form factor profiles of diesel, premixed LGO, and neat LGO.

The fraction of heat released is expressed by the non-dimensional equation as follows:

$$x = 1 - \exp\left\{-a\left[\frac{\theta - \theta_i}{\Delta\theta_c}\right]^{m+1}\right\} \tag{5}$$

where $\Delta\theta_c$ is the duration of combustion in terms of crank angle, θ the crank angle at any instant, θ_i the crank angle at the start of combustion, a the parameter that characterizes the completeness of combustion (for MFB = 0.9, a = 2.3026), and m the form factor.

$$m = f\{\theta_{10}, \theta_{90}\} = \frac{\ln\left(\frac{0.1}{0.9}\right)}{\ln\left(\frac{\theta_{90}-\theta_i}{\theta_{10}-\theta_i}\right)} \tag{6}$$

The plot 9 (a) has a characteristic S-shape. From the plot, the rate at which fuel–air mixture burns grows from zero (start of combustion) and then tends exponentially to one (end of combustion). Moreover, from Fig. 9(b) it can be noticed that the form factor values are in the range of 0.35–0.46 for diesel, 5% premixed ratio, 10% premixed ratio, and neat LGO, respectively. The parameter 'm' characterizes the rate of combustion. The small value of 'm' means a high rate at the beginning of combustion, while large value of 'm' signifies a high rate by the end of combustion.

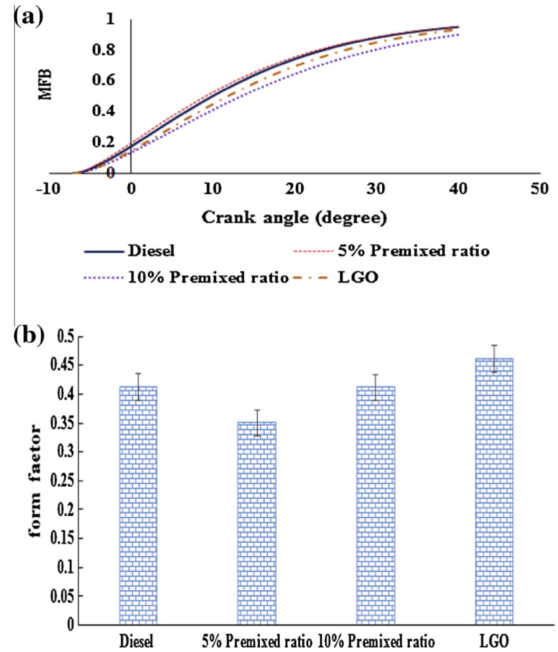

Figure 9 (a) Mass fraction burned and (b) form factor of fitted Wiebe function.

4. Conclusions

In this work, the combustion characteristics of neat and premixed LGO in a modified single-cylinder air-cooled CI engine operated at a maximum load of 3.3 kW were profoundly studied. Based on the experimental investigations, the following observations are drawn:

- LGO can be used as a sole fuel in CI engine without any pre-treatment processes such as transesterification, pyrolysis or emulsion.
- The shorter ignition delay period was evident for premixed and neat LGO than neat diesel.
- Although maximum work per cycle reduced for neat LGO, the combination of slower heat-release rate and lower maximum rate of pressure rise might cause lower mechanical stress in the crank drive when compared to diesel operation. Therefore, low combustion noise can be achieved with neat LGO operation.
- The experimental investigation on PCCI-DI dual fuel mode did not result in better performance when compared to diesel combustion. However, the emission reductions (especially NO_x and smoke) will be the primary area of investigation and area of interest.
- Current views on lemongrass oil combustion characteristics disclose that, in general, they can only represent alternative to conventional diesel combustion. However, the details on how maximum work per cycle can be improved and future emission standards can be met are not addressed.
- On this last concern scientific advancements are fundamentally required in current engine technology to address the global issue on depletion of easily accessible fossil fuels.

References

[1] Amin Talebian-Kiakalaieh, Nor AishahSaidina Amin, Hossein Mazaheri, A review on novel processes of biodiesel production from waste cooking oil, Appl. Energy 104 (2013) 683–710.

[2] H. An, W.M. Yang, A. Maghbouli, J. Li, S.K. Chou, K.J. Chua, Performance, combustion and emission characteristics of biodiesel derived from waste cooking oils, Appl. Energy (2013), http://dx.doi.org/10.1016/j.apenergy.2012.12.044.

[3] J.H. Van Gerpen, B.B. He, 14 – Biodiesel and renewable diesel production methods, in: Keith Waldron (Ed.), Advances in Biorefineries, vol. 441, Woodhead Publishing, 2014, ISBN: 9780857095213.

[4] L.E. Rincón, J.J. Jaramillo, C.A. Cardona, Comparison of feedstocks and technologies for biodiesel production: an environmental and techno-economic evaluation, Renew. Energy 69 (2014) 479–487.

[5] A. Carrero, Á. Pérez, 5 – Advances in biodiesel quality control, characterisation and standards development, in: Rafael Luque, Juan A. Melero (Eds.), Advances in Biodiesel Production. Woodhead Publishing Series in Energy, Woodhead Publishing, 2012, http://dx.doi.org/10.1533/9780857095862.1.91, p. 91, ISBN: 9780857091178.

[6] Roy Murari Mohan, Wang Wilson, Bujold Justin, Biodiesel production and comparison of emissions of a DI diesel engine fueled by biodiesel-diesel and canola oil-diesel blends at high idling operations, Appl. Energy (2013) 198–208.

[7] R. Alenezi, R.C.D. Santos, S. Raymahasay, G.A. Leeke, Improved biodiesel manufacture at low temperature and short reaction time, Renew. Energy 53 (2013) 242–248.

[8] www.renewable energy world.com.

[9] S.K. Karmee, Chadha Anju, Preparation of bio diesel from crude oil of Pongamiapinnata, Bioresource Technol. 96 (2005) 1425–1429.

[10] A. Gnanaprakasam, V.M. Sivakumar, A. Surendhar, M. Thirumarimurugan, T. Kannadasan, Recent strategy of biodiesel production from waste cooking oil and process influencing parameters: a review, Energy (2013), http://dx.doi.org/10.1155/2013/926392.

[11] K. Soloman Binu, S. Prabhakar, S. Aque Ahmed Ashf, C. Vikram Jagdeesh, Performance test for lemon grass oil in single cylinder diesel engines source, J. Eng. Appl. Sci. 8 (2013) 455–458.

[12] Valtcho D. Zheljazkov, Charles L. Cantrel, Tess Astatkie, Jeffery B. Cannon, Lemongrass Productivity, Oil Content, and Composition as a Function of Nitrogen, Sulfur, and Harvest Time. http://dx.doi.org/10.2134/agronj2010.0446.

[13] Hua Zhao, HCCI and CAI Engines for the Automotive Industry, Wood Head Publishing, CRC Press, Cambridge, England, 2007.

[14] B. Premanand, T. Senthil Kumar, S. Sivaprakasam, C.G. Saravanan, Combustion and emission characteristics of DIdiesel engine using bio diesel, in: 19th National Conference on IC Engine and Combustion (The Combustion Institute (Indian Section)), 2005, p. 113.

[15] Ya-fen Lin, G. Wu Yo-Ping, C.T. Chang, Combustion characteristics of waste oil produced bio-diesel, diesel fuel blends, Fuel 86 (2007) 1772–1789.

[16] A. Demirbas, Importance of bio diesel as transportation fuel, Int. J. Energy Policy 35 (2007) 4661.

[17] A.K. Agarwal, Bio fuels (alcohols and bio diesel) applications as fuels for internal combustion engines, Int. J. Prog. Energy Combust. 33 (2007) 233.

[18] A.K. Babu, G. Devaradjane, Vegetable Oils and their derivatives as Fuels for CI Engine: An Overview, SAE Technical Paper 2003-01-0767, pp. 406–419.

[19] J.B. Heywood, Internal Combustion Engine Fundamentals, 1989, ISBN: 0-07-100499-8.

[20] M. Gumus, A comprehensive experimental investigation of combustion and heat-release characteristics of a biodiesel (hazelnut kernel oil methyl ester) fueled direct injection compression ignition engine, Fuel 89 (2010) 2802–2814.

[21] D.C. Rakopoulos, C.D. Rakopoulos, E.C. Kakaras, E.G. Giakoumis, Effects of ethanol diesel blends on the performance and exhaust emissions of a heavy duty DI diesel engine, Energy Convers. Manage. 49 (2008) 3155–3162.

[22] El-Kassaby Medhat nemit-allah, Experimental investigations of ignition delay period and performance of a diesel engine operated with Jatropha oil biodiesel, Alexandria Eng. 52 (2013) 141–149.

[23] M. Senthil kumar, A. Ramesh, B. Nagalingam, Complete Vegetable Oil Fueled Dual Fuel Compression Ignition Engine, SAE Technical Paper 2001-28-0067.

[24] J. Nazar, A. Ramesh, R.P. Sharma, Performance and Emission Studies of Use SVO and Bio Diesel from Different Indian Feed Stock, SAE Technical Paper. No. 2004-28-071.

[25] N.R. Banapurmath, P.G. Tewari, R.S. Hosmath, Performance and emission characteristics of a DI compression ignition engine operated on Honge, Jatropha and Sesame oil Methyl esters, Renew. Energy 33 (2007) 1982–1988.